Journal of Solid State Chemistry **142,** 108–112 (1999)
Article ID jssc.1998.8010, available online at http://www.idealibrary.com on IDEAL®

Optical Spectroscopy of Nd^{3+} Ions in $CsGd_2F_7$ Host

C. L. M. de Barros and R. B. Barthem[1]

Instituto de Física - UFRJ, Cx. P. 68528, CEP 21945-970 Rio de Janeiro, RJ, Brazil

and

N. M. Khaidukov

Institute of General and Inorganic Chemistry, Russian Academy of Sciences, 117071, Moscow, Russia

Received July 2, 1997; in revised form January 14, 1998; accepted August 20, 1998

Optical spectroscopic studies of the compound $CsGd_2F_7:Nd^{3+}$ have been carried out with the purpose of determining the lanthanide ion site luminescence properties. These studies have been made at low temperatures with crystals containing 0.3 to 3 at.% of Nd^{3+} ion substituting for Gd^{3+} ions. The experimental results discussed here are based on the analysis of the absorption, fluorescence, and excitation spectra. We have shown the presence of seven absorber centers disposed in four groups. Three of them exhibit a substructure composed of two sites each. These Nd^{3+} ion centers have been correlated with known crystallographic sites.

INTRODUCTION

Presently, more than 70 fluoride crystals with ordered structures are used as laser host matrices (1, 2) for various lanthanide ions, alkaline earth, and transition metals. A special case for the practical application of these new materials, as noted in Ref. (3), is the possibility of the creation of various polyfunctional laser devices.

Fluoride compounds MLn_2F_7 (M = K, Rb, Tl, and Cs; Ln = Y, Lu, and Gd) can form various structural arrangements. According to preliminary studies (2–7), $CsGd_2F_7$ has the same crystallographic characteristics as KEr_2F_7, i.e., hexagonal structure and space group D_6^6–$P6_322$. Nevertheless, Aleonard *et al.* (4) in their analysis of KEr_2F_7 and its high temperature phase (β-KEr_2F_7) found strong analogies between the two compounds based on single crystal diffractometer measurements for β-KEr_2F_7.

With the purpose of illustrating and supporting the analysis and identification of sites of $CsGd_2F_7$, we show the β-KEr_2F_7 structure (4) in Fig. 1. The fluorine atoms form the vertices of the polyhedra. The erbium ions are located inside the polyhedra; three of them, Er(1), Er(2), and Er(3), are coordinated antiprismatically, and the fourth, Er(4), corresponds to a distorted cube with each of the adjacent four faces rotated in its plane. Two antiprisms and the dodecahedron share two of their faces to form the $(Er_3F_{17})^{8-}$ groups. These groups are bidimensionally linked, and the planes that they form are joined together by the third antiprism. A three-dimensional network is then produced, creating channels in which the potassium ions are located.

This work presents and analyzes the results of an optical study of Nd^{3+} ions diluted in single crystals of $CsGd_2F_7$, considering this host to be isostructural with KEr_2F_7. In this way four types of erbium sites have been observed.

EXPERIMENTAL PROCEDURE

In recent years, high-temperature methods for crystal growth, like Bridgman-Stockbarger and Czochralski, have ceased to allow the fast search for new lasing fluorides. One likely reason is the fact that many new laser compounds have polymorphic phase transitions at high temperatures (5). Using low-temperature methods for growing crystals, in particular the hydrothermal method (6), Khaidukov and others workers got positive results searching for new prospective fluoride laser hosts (7).

$CsGd_2F_7$ single crystals were grown by the hydrothermal synthesis technique in the temperature interval between 450 and 700°C and the pressure interval between 100 and 150 MPa, applied for 15 to 20 days, under the chemical interaction of the oxide compound $(1-x)Gd_2O_3$–xNd_2O_3 in aqueous CsF solution. The growth of single-phase samples was controlled as in Ref. (8). Optically clear, single crystals were obtained, with thicknesses of about 1 mm and

[1] To whom correspondence should be addressed. E-mail: barthem@if.ufrj.br.

0022-4596/99 $30.00

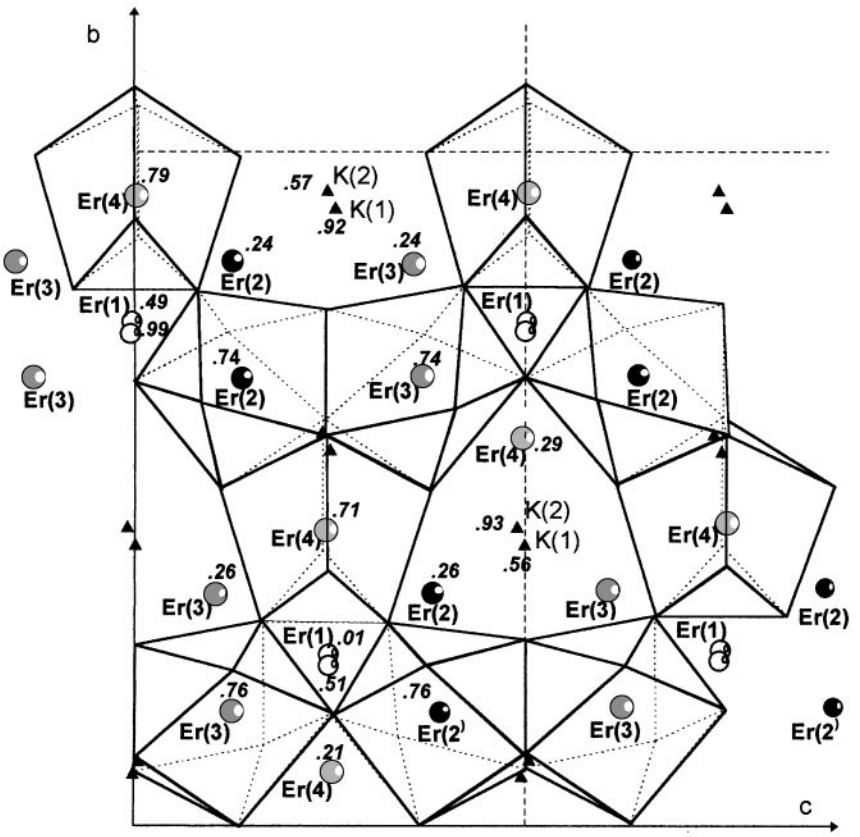

FIG. 1. Projection (100) of the β-KEr_2F_7 structure. The erbium sites identified crystallographically (4) are indicated. The polyhedral vertices are formed by fluoride ions. The erbium ions are inside the polyhedra; three of them, Er(1), Er(2), and Er(3), are antiprisms and the fourth, Er(4), corresponds to a distorted cube where four of their adjacent faces suffer, each one, a rotation in their plane. The potassium ions are inside another kind of polyhedron formed by 9–11 fluoride ions with variable distances between them.

containing 0.3, 1, and 3 at.% Nd^{3+} ions in the Gd^{3+} ion sites.

Absorption, excitation, and fluorescence spectra from $CsGd_2F_7:Nd^{3+}$ crystals were obtained. To benefit from the narrowness of the inhomogeneous energy transitions and to reduce phonon effects, all the experiments have been conducted using low-temperature techniques at liquid helium or nitrogen temperature using a Janis ST-100 gas flow cryostat.

The luminescence and absorption spectra were obtained with a 2061 MacPherson spectrometer and a Hamamatsu (Model 128) photomultiplier. Laser selective excitation and excitation spectra were produced with a home-made dye laser (8) pumped by a Nd:YAG pulsed laser Spektrum Model Speser 603. An EG&G PAR Instrumentation Model 5209 lock-in and a Tektronix Model TDS 350 digital oscilloscope were used to acquire and produce the primary signal treatment. For these experiments, a microcomputer was interfaced to the equipment in order to control the spectrometer or laser scanning and to register the spectra.

RESULTS

Absorption spectra from Nd^{3+} ions in $CsGd_2F_7:Nd^{3+}$ (1 at.%) crystals are presented in Figs. 2a and 2b at $T = 4$ K and 2c at $T = 77$ K. They correspond to transitions from the ground-state $^4I_{9/2}$ multiplet to the $^2P_{1/2}$ level. The absorption lines observed in these spectra are disposed in four groups characterized by polarization properties and line separation. Three of them are constituted by pairs of lines designated P_2 and P_3, P_4 and P_5, and P_6 and P_7. The fourth group is formed by only one line denoted P_1. While P_6 is found at 6 cm^{-1} away from P_7, P_5 and P_4 are separated by 3 cm^{-1} and P_3 and P_2 are 7 cm^{-1} away from each other. In the polarized absorption spectra (Figs. 2b and 2c), the group characteristics of the pair lines are more evident. While the intensities of lines P_6 and P_7 increase when the polarization changes from σ ($E \perp c$) to π ($E//c$), the intensities of lines P_2 and P_3 decrease as those of lines P_4 and P_5. The P_1 line seems unaffected by the polarization changes.

Polarized absorption spectra in the region of the $^4I_{9/2} \rightarrow {}^4F_{3/2}$ transitions, observed with 0.3, 1, and 3 at.%

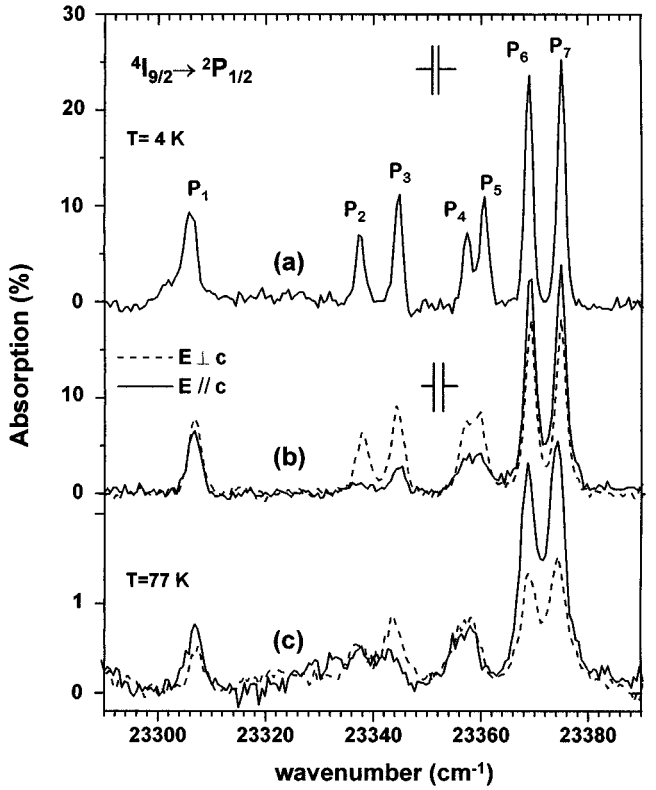

FIG. 2. Absorption spectra from $CsGd_2F_7:Nd^{3+}$ (1 at.%) in the blue region ($^4I_{9/2} \rightarrow {}^2P_{1/2}$). (a) Nonpolarized spectrum at $T = 4$ K, (b) polarized spectra at $T = 4$ K, and (c) polarized spectra at $T = 77$ K.

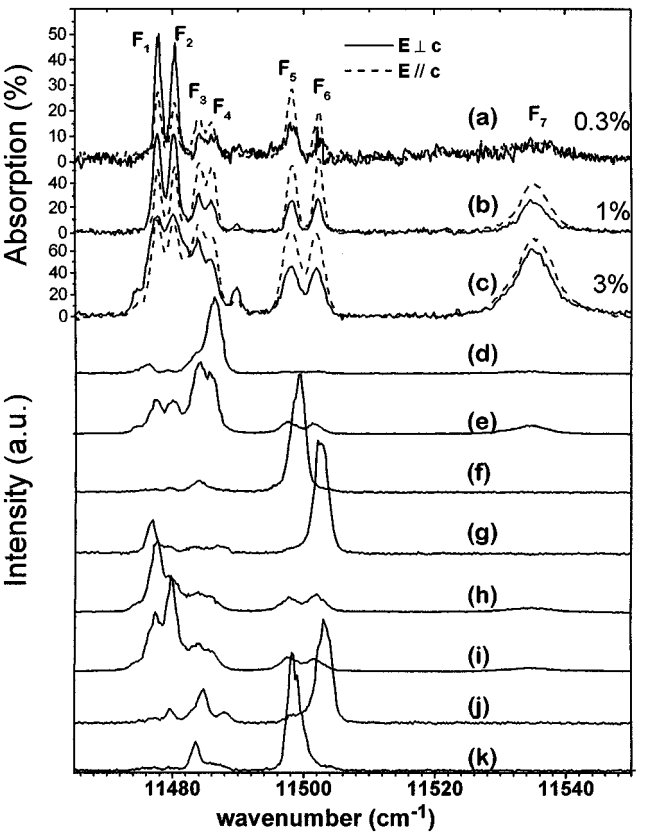

FIG. 3. Polarized absorption spectra (a, b, and c) from $CsGd_2F_7:Nd^{3+}$ at $T = 4$ K, near the infrared region showing the transitions $^4I_{9/2} \rightarrow {}^4F_{3/2}$. The Nd^{3+} concentrations are (a) 0.3, (b) 1, and (c) 3 at.%. Selective luminescence spectra (d to k) from $CsGd_2F_7:Nd^{3+}$ (3 at.%) crystal at $T = 4$ K. These spectra have been obtained after $^4I_{9/2} \rightarrow {}^4G_{5/2}$ dye-laser excitation ($\Delta\sigma = 0.2$ cm^{-1}) on (d) G_1 center line, (e) G_1 high energy border line, (f) G_2, (g) G_3, (h) G_4, (i) G_5, (j) G_6, and (k) G_7 lines. The luminescent signals have been integrated over time.

Nd^{3+} doped samples at $T = 4$ K, are detailed in Figs. 3a, 3b, and 3c, respectively. We observe that the intensities of some groups of lines are coupled, suffering the same proportional variation with applied polarization, like F_1 and F_2, F_3 and F_4, and F_5 and F_6. The F_7 line is much more diffuse, and its shape has no similarities with those of the other lines. The energy distance between the lines in each pair is presented in Table 1, together with the results obtained for the other transitions analyzed in this paper.

The $^4I_{9/2} \rightarrow {}^4G_{5/2} + {}^2G_{7/2}$ transitions occur in the orange spectral region. The polarized absorption spectra around the lower energy lines of these transitions, for 0.3, 1, and 3 at.% Nd^{3+} doped $CsGd_2F_7$ crystals at $T = 4$ K, are presented in Figs. 4a, 4b, and 4c, respectively. The lines shown are labeled from G_1 to G_{11}. As the $^4G_{5/2}$ multiplet could be split on three levels, it would be possible to observe, following the number of lines presented in Figs. 2 and 3, up to $3 \times 7 = 21$ lines! The first 7 lines, from G_1 to G_7, present practically the same linewidth, while the linewidths of G_8 to G_{11} are larger. The narrow lines, from G_1 to G_7, have been excited selectively, by a tunable dye laser, and the luminescence observed from the transition $^4F_{3/2} \rightarrow {}^4I_{9/2}$ presented in Fig. 3, spectra (d) to (k), for the 3 at.% Nd^{3+} doped crystal at $T = 4$ K. Spectra (d) and (e) in Fig. 3 refer to the G_1 excitation line in two increasing energy positions. The other spectra, (f) to (k), in Fig. 3 correspond to the line excitation from G_2 to G_7, respectively.

TABLE 1
Energy Separation between Lines in the $^2P_{1/2}$ (P_i Lines), $^4F_{3/2}$ (F_i Lines), and $^4F_{5/2}$ (G_i Lines)

Line pair	ΔE (cm^{-1})
P_2–P_3	7.1
P_4–P_5	3.3
P_6–P_7	6.0
F_1–F_2	2.5
F_3–F_4	2.1
F_5–F_6	3.4
F'_5–F'_6	5.2
G_2–G_3	24.1
G_4–G_5	3.5
G_6–G_7	7.7

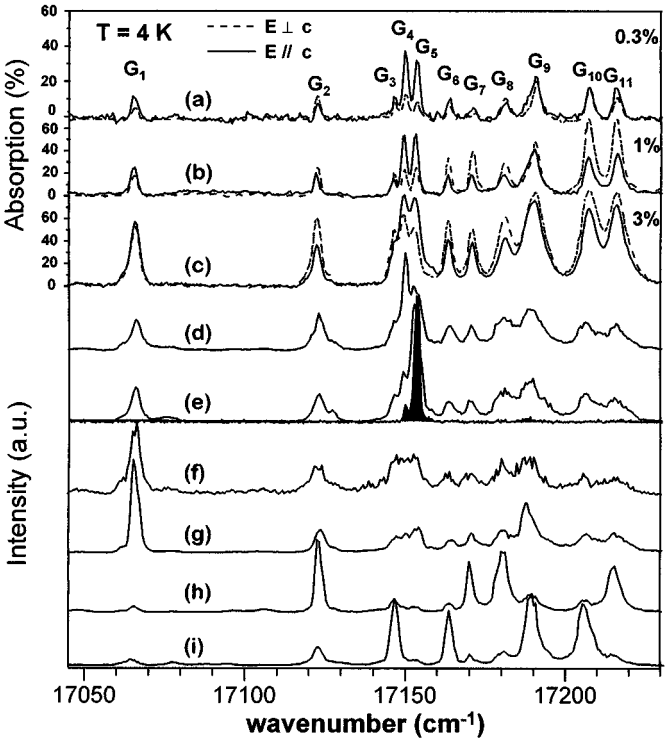

FIG. 4. Polarized absorption spectra (a, b, and c) from $CsGd_2F_7:Nd^{3+}$ at $T = 4$ K, in the yellow region showing the transitions $^4I_{9/2} \rightarrow {}^4G_{5/2}$. The Nd^{3+} concentrations are (a) 0.3, (b) 1, and (c) 3 at.%. Excitation spectra (d to i) from $CsGd_2F_7:Nd^{3+}$ (3 at.%) crystal at $T = 4$ K of the $^4F_{3/2} \rightarrow {}^4I_{9/2}$ luminescence lines ($\Delta\sigma = 2\ cm^{-1}$) (d) F_1, (e) F_2 (0.3% in shadow), (f) F_3, (g) F_4, (h) F_5, and (i) F_6. The luminescent signals have been integrated over time.

The correspondence between the $^4G_{5/2}$ and the $^4F_{3/2}$ levels, obtained with the selective line excitation luminescences presented in spectra (d) to (k) in Fig. 3, can also be established in the inverse sense from $^4F_{3/2}$ luminescence to $^4G_{5/2}$ excitation. Spectra (d) to (i) in Fig. 4 present the excitation spectra of the F_1 to F_6 luminescence lines between the $^4I_{9/2} \rightarrow {}^4G_{5/2}$ transitions, obtained from the same 3 at.% Nd^{3+} doped crystal at $T = 4$ K. The higher Nd^{3+} concentration has been chosen in order to obtain larger intensities. However, greater Nd^{3+} concentrations increase site transfer and, as a consequence, a larger number of satellite lines appear. Dynamical studies of quenched and upconversion luminescence are under study and will be published later. The shadow peaks in spectrum e of Fig. 4 represent the 0.3 at.% Nd^{3+} concentration excitation spectrum for the same F_2 luminescence line.

The excitation spectrum for the F_7 luminescence line has also been recorded, yielding a very small line intensity. The luminescence spectra (d) to (k) in Fig. 3 exhibit low F_7 line intensities, in accord with the excitation spectrum result.

ANALYSIS

The origin of multiple lines is the first aspect to be discussed. As the $^2P_{1/2}$ level is significantly isolated from other multiplets and it offers only one possibility for transitions, it constitutes a good probe for analyzing the line multiplicity. The relative intensities of these lines (P_i, $i = 1, 2, \ldots, 7$) are practically insensitive to a variation of temperature between 4 and 77 K, as shown in spectra (b) and (c) in Fig. 2. As the population of the $^4I_{9/2}$ multiplet levels is temperature dependent, the $^4I_{9/2}$ excited levels cannot be the cause of these optical transitions. Besides, at 4 K, only the levels of the $^4I_{9/2}$ multiplet located below $8\ cm^{-1}$ above the ground state can be significantly populated.[2] The only way for the excited $^4I_{9/2}$ multiplet levels to be present among these lines would be on the pairs of lines $P_2 + P_3$, $P_4 + P_5$, and $P_6 + P_7$. However, if these pairs originate from the $^4I_{9/2}$ multiplet, the energy separation between theirs lines should be the same for all the other multiplet transitions. This is not the case, as shown in Table 1. Thus, we must conclude that all seven lines have origin on the $^4I_{9/2}{}^{(0)}$ ground state and that each one is associated with a different type of Nd^{3+} ion site. Kaminskii *et al.* (10) point out the existence of six centers.

In order to obtain the correlation between the transitions from $^4I_{9/2}{}^{(0)}$ to different multiplets (11) it is necessarily an internal transfer process, with in the excitated Nd^{3+} ion, that could change the excitation from one multiplet to another. The $^2P_{1/2}$ level cannot offer this process because of the large separation from the next multiplet, $^4G_{11/2}$, which is more than $2000\ cm^{-1}$ lower in energy. The $^4G_{5/2}$ multiplet, on the other hand, is quickly deexcited to the $^4F_{3/2}{}^{(0)}$ lower level multiplet, a well-known luminescent level. Spectra (d) to (k) in Fig. 3 indicate that the $^4F_{3/2}{}^{(0)} \rightarrow {}^4I_{9/2}{}^{(0)}$ lines (F_i) are linked to the $^4I_{9/2}{}^{(0)} \rightarrow {}^4G_{5/2}{}^{(0)}$ lines (G_i). These correlations are corroborated by the excitation spectra (d) to (i) in Fig. 4, which indicate, in the inverse sense, that the $^4I_{9/2}{}^{(0)} \rightarrow {}^4G_{5/2}{}^{(0)}$ lines (G_i) are associated with the $^4F_{3/2}{}^{(0)} \rightarrow {}^4I_{9/2}{}^{(0)}$ luminescent lines (F_i). Only the more intense line luminescence corresponds to the same site process. The others have been identified as site–site transfers by dynamical properties (not presented here) or by changing the Nd^{3+} concentration, as shown in spectrum (e) in Fig. 4.

Three important remarks follow. The first one concerns the F_7 line. As shown in the luminescence spectra (a) to (k) in Fig. 3, this line appears only on the absorption spectra. It must be originated on the $^4F_{3/2}{}^{(1)}$ level, the first excited state of the $^4F_{3/2}$ multiplet. Its large line width is consistent with this hypothesis. The second remark addresses the F_3 and F_4 lines. Both lines have been correlated to the same line G_1 in the $^4I_{9/2} \rightarrow {}^4G_{5/2}$ spectrum. The excitation spectra (f) and (g) in Fig. 4 suggest that the line G_1 is composed, actually, of

[2] For $T = 4$ K and $E = 10\ cm^{-1}$, $e^{-E/kT} = 2.7\%$.

TABLE 2
Line Correlation between the Observed Transitions from the Ground-State $^4I_{9/2}{}^{(0)}$ to the Low Levels of the Excited Multiplets $^4G_{5/2}{}^{(0)}$ (Lines G_i), $^4F_{3/2}$ (F_i), and $^2P_{1/2}$ (P_i)

	Line transitions		
Site type	$^4I_{9/2} \rightarrow {}^4G_{5/2}$	$^4I_{9/2} \leftrightarrow {}^4F_{3/2}$	$^4I_{9/2} \rightarrow {}^4P_{1/2}$
Er(4)	G_1	$F_{3,4}$	P_1
Er(2) or (3)	G_2	F_5	P_2 or P_3
Er(2) or (3)	G_3	F_6	P_2 or P_3
Er(1)	G_4	F_1	P_6 or P_7
Er(1)	G_5	F_2	P_6 or P_7
Er(2) or (3)	G_6	F'_6	P_4 or P_5
Er(2) or (3)	G_7	F'_5	P_4 or P_5

Note. The site assignments for the equivalent β-KEr_2F_7 structure (4) are identified by the Er-labeled sites.

two nonresolved lines. The $^4F_{3/2}$ luminescence (d) and (e) in Fig. 3 corroborate this idea. For these two lines we could attribute one Nd^{3+} site to each one, which would result in eight sites. However, as the G_1 line cannot be resolved into two lines, and the transitions involving the $^2P_{1/2}$ level are limited to seven, we limit the number of observed sites to seven. The third remark involves lines F_5 and F_6. Each one appears to be composed of two lines separated by about 1 cm^{-1}. The pairs $F_5 + F_6$ and $F'_5 + F'_6$ correlated with the pairs $G_2 + G_3$ and $G_7 + G_6$ and have their lines separated by 3.4 and 5.2 cm^{-1} ($\pm 10\%$), respectively.

The lines on these two spectrum ensembles exhibit also the same group properties, in agreement with the abovementioned correlations. These properties are the proximity and the intensity dependence with polarization. These observations lead us to propose a correlation with the lines from the $^4I_{9/2}{}^{(0)} \rightarrow {}^2P_{1/2}$ transitions. These observations are summarized in the Table 2.

Taking into account these considerations, we present a site crystal assignment for the seven lines observed. For the β-KEr_2F_7 structure (4), proposed to be similar to the $CsGd_2F_7$ structure, there are four types of Er^{3+} sites. Two of them are very similar, as can be seen in Fig. 1. The Er(2) and Er(3) sites have nearly the same form, one being almost the reflection of the other. Because line pairs $P_2 + P_3$ and $P_4 + P_5$ in the $^4I_{9/2}{}^{(0)} \rightarrow {}^2P_{1/2}$ absorption spectrum, and the lines pairs $G_2 + G_3$ and $G_6 + G_7$ in the $^4I_{9/2}{}^{(0)} \rightarrow {}^4G_{5/2}$ spectrum correlated with the line pairs $F_5 + F_6$ and $F'_5 + F'_6$ in the $^4I_{9/2}{}^{(0)} \rightarrow {}^4F_{3/2}$ spectrum, all have the same characteristics, we propose that these sites give origin to these lines. In the $CsGd_2F_7$ crystal the equivalent sites, Gd(2) and Gd(3), must be subjected to new distortions in order to produce four distinct sites, Gd(2′), Gd(2″), Gd(3′), and Gd(3″), which should retain many of the original site characteristics.

Like sites Er(2) and Er(3), the Er(1) site is also coordinated antiprismatically. Because the line pair $P_6 + P_7$, and the correlated line pairs $G_4 + G_5$ and $F_1 + F_2$, have many of the properties assigned to the lines associated with the Er(2) and Er(3) sites, we link them to the Er(1) type site. Like the Er(2) and Er(3) sites, the Gd(1) site must also be subjected to some distortion in order to produce two distinct sites, Gd(1′) and Gd(1″), one for each line P_6 and P_7. The last site, Er(4), should be assigned to the P_1 line which is correlated to the G_1 and $F_{3,4}$ lines. Er(4) corresponds to a totally different site, in the form of a distorted cube. This difference might explain why the equivalent site Gd(4) has not been converted, at least in an observable way, into two new sites, as occurred with the other sites.

CONCLUSION

In our study of the $CsGd_2F_7:Nd^{3+}$ compound, via low-temperature absorption spectra, we observed four line groups whose common characteristics are observed in several transitions. These lines were related to the crystallographic sites already identified in the literature (4). The energy differences between the same Nd^{3+} transitions at different sites reach several tens of cm^{-1}. Yet we proposed that three of these sites have a substructure composed of two sites each. These substructures cause modifications in the transition energies by only a few cm^{-1}. Based on our analysis, the total number of sites discerned and identified is seven.

ACKNOWLEDGMENTS

The authors thank CNPq, FINEP, and José Bonifácio Foundation (FUJB) for the financial support given to this work. We are grateful to Prof. S. de Souza Barros for comments which improved the paper.

REFERENCES

1. A. Kaminskii, N. M. Khaidukov, W. Koeckner, and H. R. Verdun, *Phys. Status Solidi A* **132,** K105 (1992).
2. A. A. Kaminskii, H. R. Verdum, and N. M. Khaidukov, *Dokl. Akad. Nauk*. **328,** 181 (1993).
3. I. S. Rez, *Sov. J. Quantum Electron.* **13,** 2071 (1986).
4. S. Aleonard, Y. Le Fur, M. F. Gorius, and M. Th Roux, *J. Solid State Chem.* **34,** 79 (1980).
5. O. Greis and J. M. Haschke, "Handbook on the Physics and Chemistry of Rare Earths," Vol. 5, p. 387. North Holland, 1989.
6. A. A. Kaminskii, L. N. Dem'yanets, S. E. Sarkisov, N. M. Khaidukov, and G. M. Safronov, *Izv. Akad. Nauk SSSR, Neorg. Mater.* **21,** 106 (1985).
7. A. A. Kaminskii and N. M. Khaidukov, *Phys. Status Solidi A* **129,** K65 (1992).
8. M. A. Dubinskii, N. M. Khaidukov, I. G. Garipov, L. M. Dem'yanets, A. K. Naumov, V. V. Semasko, and V. A. Malyusov, *J. Mod. Opt.* **37,** 1355 (1990).
9. R. B. Barthem and M. A. de Oliveira, "Resumos XIX ENFMC," p. 422. SBF, São Paulo, Brazil, 1996.
10. A. A. Kaminskii, N. M. Khaidukov, M. F. Jourbert, G. Boulon, and R. Mahiou, *Phys. Status Solidi A* **141,** K55 (1994).
11. R. B. Barthem, R. Buisson, J. C. Vial, and H. Harmand, *J. Lumin.* **34,** 295 (1986).